Supplementary Material

Synthesis of small size lead-free $Cs_3Bi_{2x}Sb_{2-2x}Br_9$ solid-solutions using a spatially confined growth method for efficient photocatalytic CO_2 reduction

Miaomiao Gao [a], Xiaolei Liu [b,*], Liwen Yin [a], Jinghang Chen [a], Zeyan Wang [a], Zhaoke Zheng [a], Yuanyuan Liu [a], Hefeng Cheng [a], Ying Dai [a], Baibiao Huang [a], Zehui Zhang [c,*], Peng Wang [a,*]

[a] State Key Laboratory of Crystal Materials, Shandong University, Jinan, 250100, China

[b] Institute of Nanophotonics, Jinan University, Guangzhou, 511443, China

[c] College of Chemistry and Materials, South-Central Minzu University, Wuhan, 430074, China

*Corresponding author:

E-mail: liuxiaolei@sdu.edu.cn (X. Liu)

E-mail: zehuizh@mail.ustc.edu.cn (Z. Zhang)

E-mail: pengwangicm@sdu.edu.cn (P. Wang)

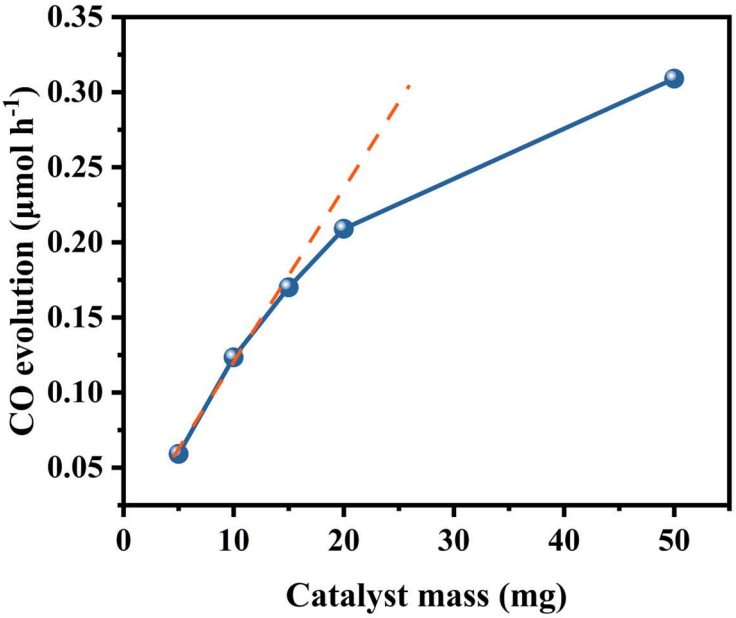

Fig. S1. Optimization of catalyst dosage.

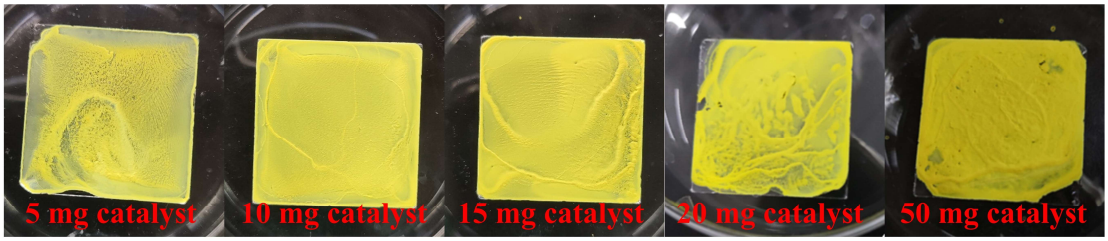

Fig. S2. The digital photographs of quartz sheets with different catalyst loading.

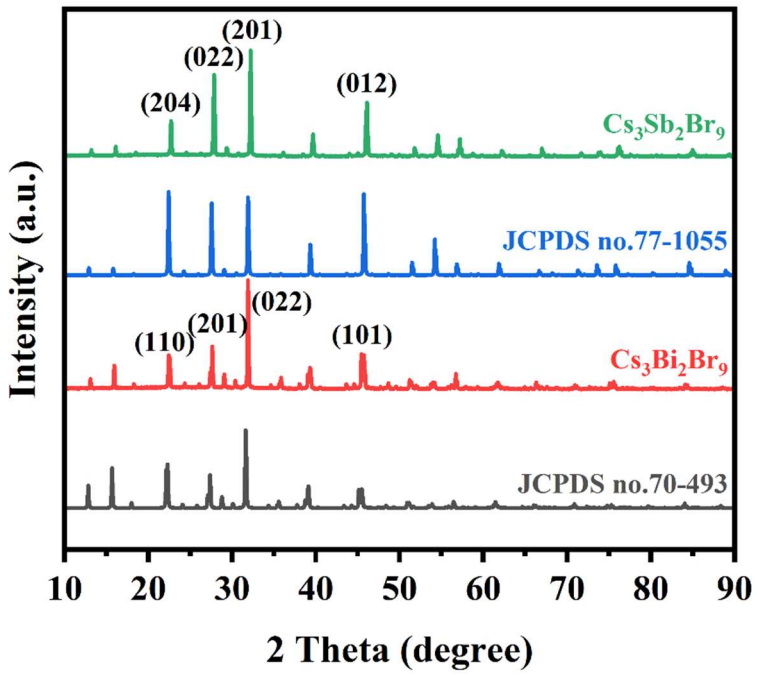

Fig. S3. XRD patterns of bulk CBB and CSB.

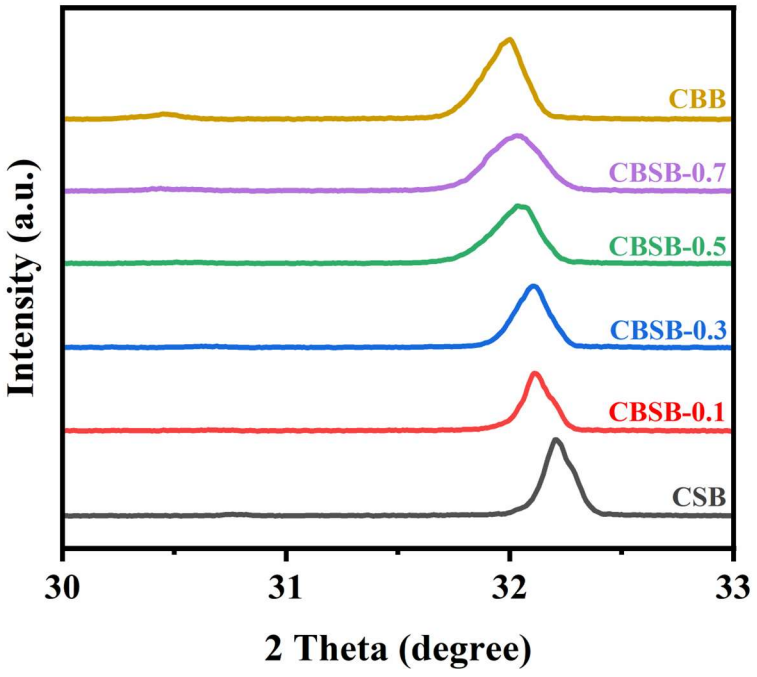

Fig. S4. The XRD patterns of bulk CBB, CSB and CBSB-X solid solutions (X = 0.1, 0.3, 0.5 and 0.7).

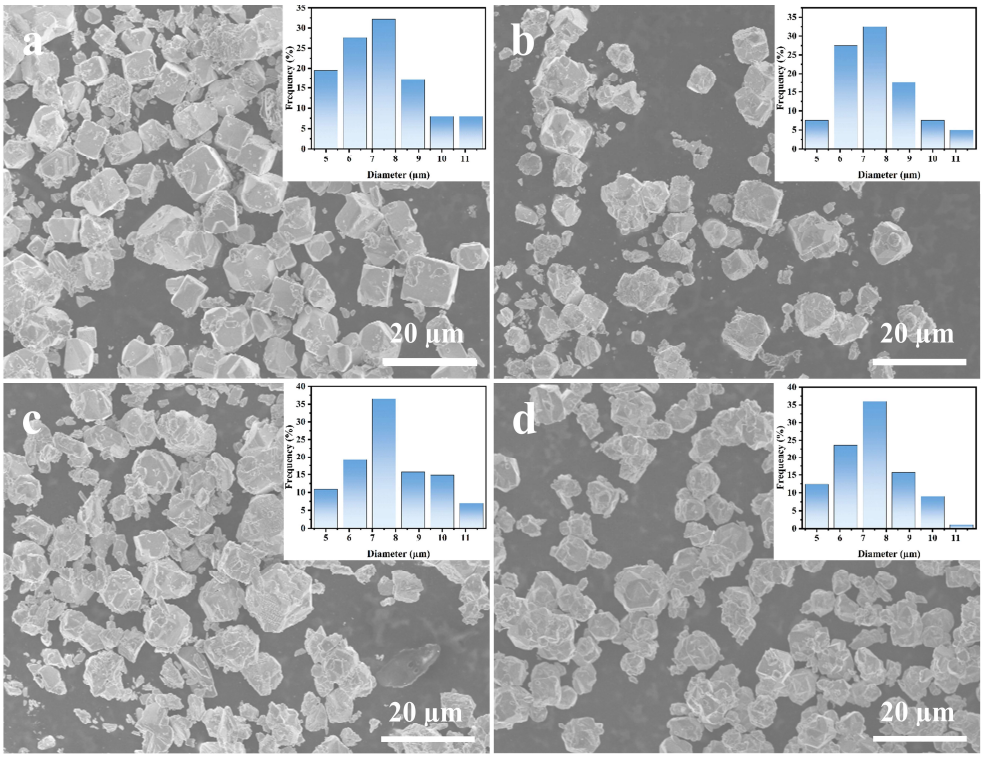

Fig. S5. SEM images of (a) CBSB-0.1, (b) CBSB-0.3, (c) CBSB-0.5, and (d) CBSB-0.7.

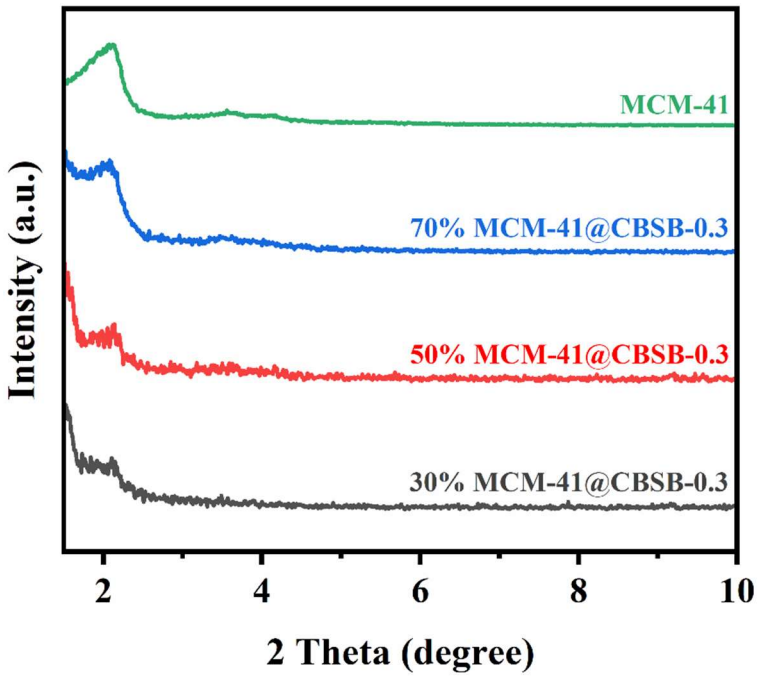

Fig. S6. The small-angle XRD patterns of the MCM-41 and a series of MCM-41@CBSB-0.3 with different weight ratios.

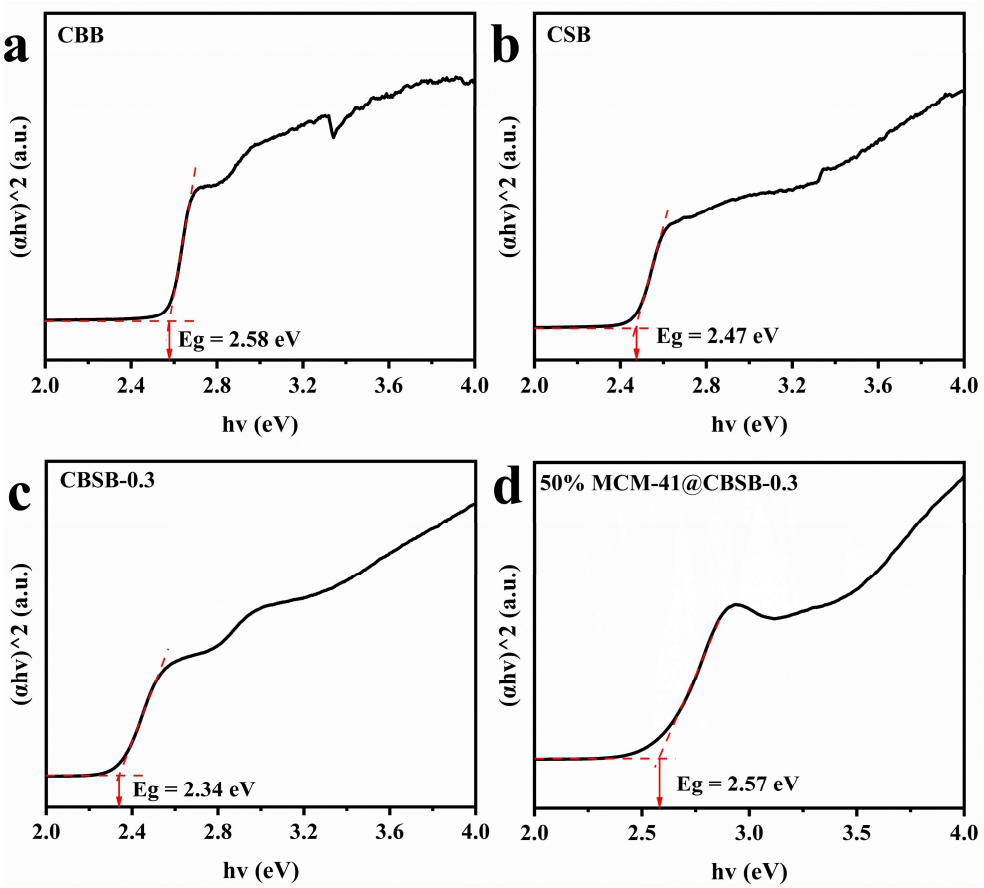

Fig. S7. The calculated optical absorption of bulk (a) CSB, (b) CBB, (c) CBSB-0.3, and (d) 50% MCM-41@CBSB-0.3.

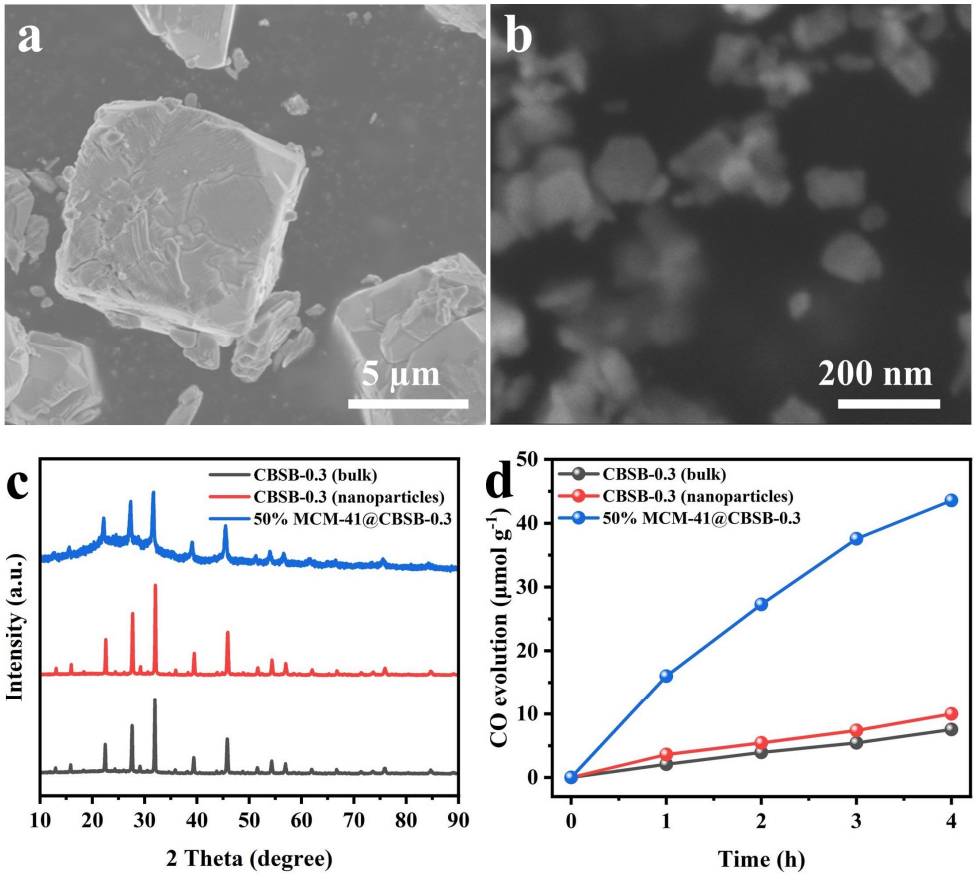

Fig. S8. SEM of (a) bulk CBSB-0.3 and (b) CBSB-0.3 nanoparticles. (c) The XRD patterns and (d) The photocatalytic performances of the bulk CBSB-0.3, CBSB-0.3 nanoparticles, and 50% MCM-41@CBSB-0.3.

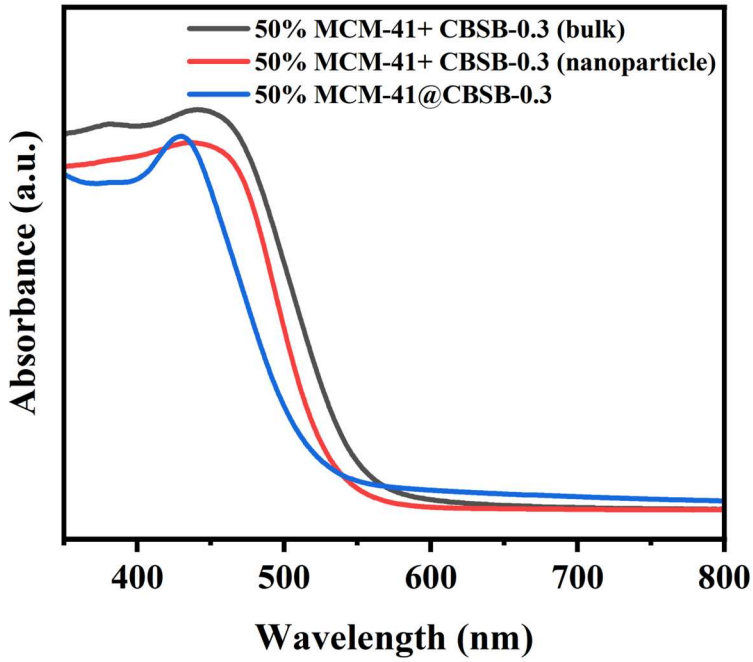

Fig. S9. UV-vis diffuse reflectance spectra of 50% MCM-41+CBSB-0.3 samples with different sizes.

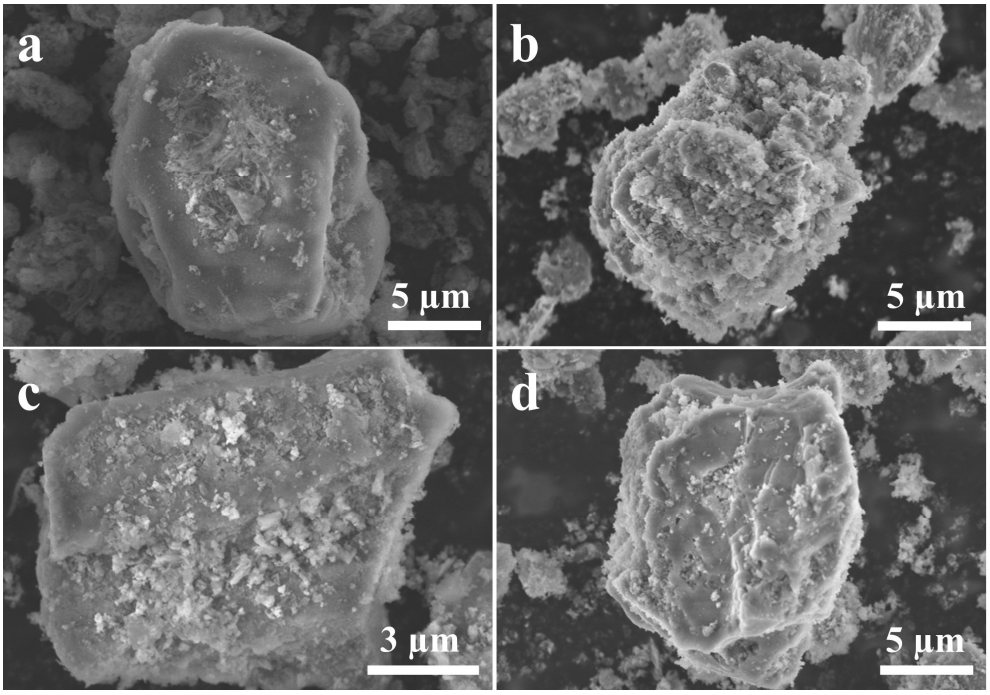

Fig. S10. SEM images of (a) MCM-41, (b) 30% MCM-41@CBSB-0.3, (c) 50% MCM-41@CBSB-0.3, (d) 70% MCM-41@CBSB-0.3.

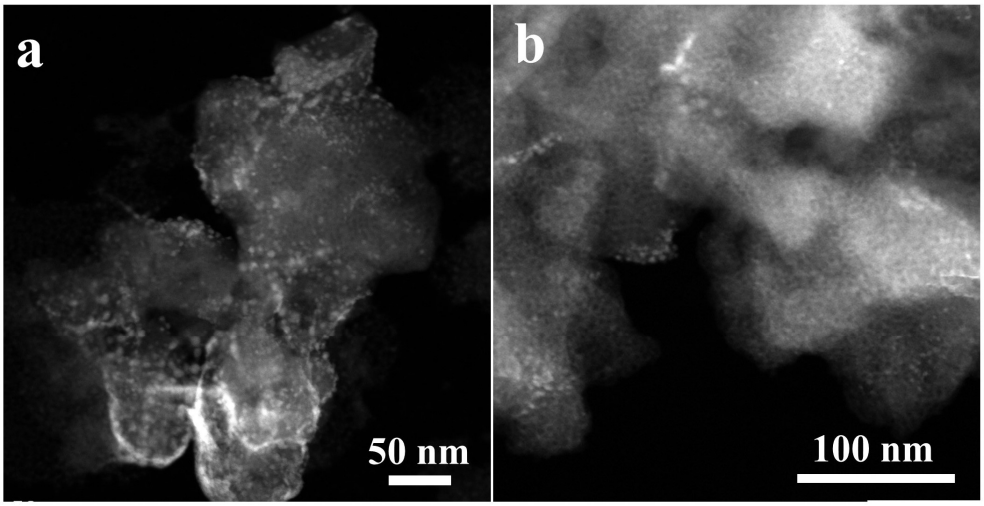

Fig. S11. TEM images of (a) 30% MCM-41@CBSB-0.3, (b) 70% MCM-41@CBSB-0.3.

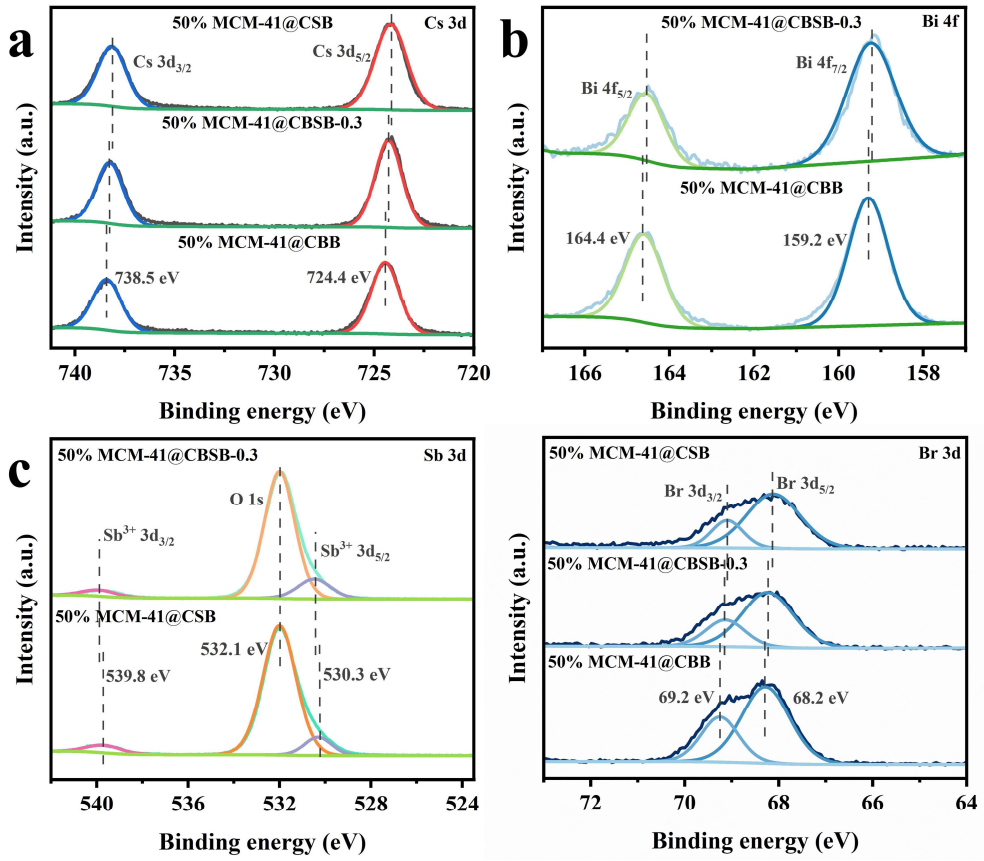

Fig. S12. The high-resolution XPS spectra of (a) Cs 3d, (b) Bi 4f, (c) Sb 3d, and (d) Br 3d of the 50% MCM-41@CBB, 50% MCM-41@CSB, and 50%

MCM-41@CBSB-0.3 samples.

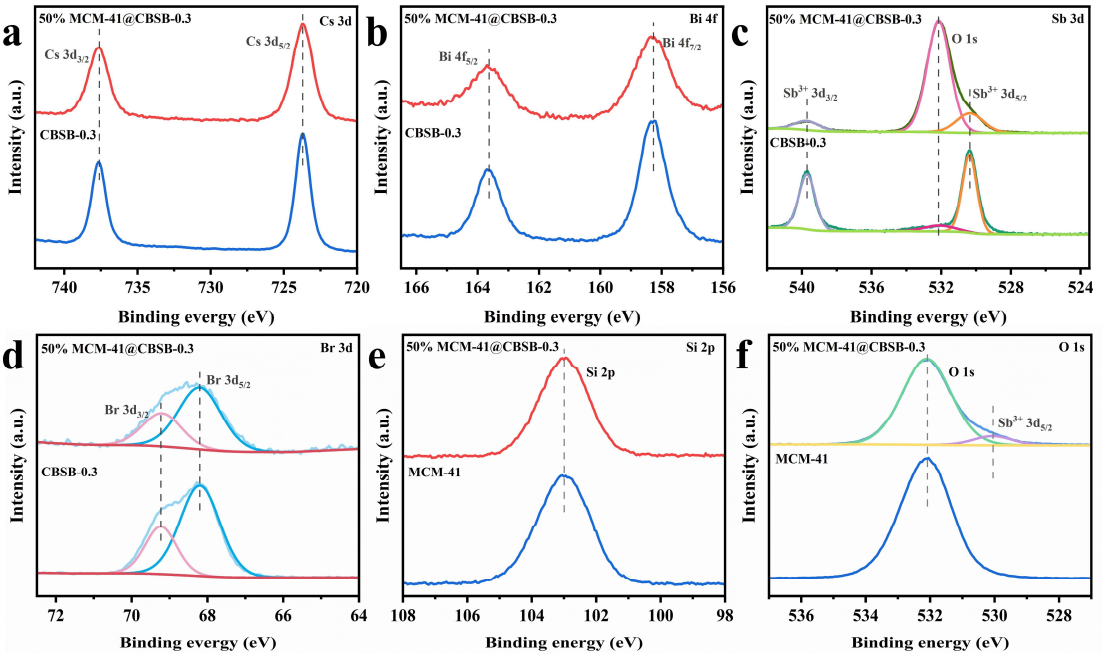

Fig. S13. The high-resolution XPS spectra of (a) Cs 3d, (b) Bi 4f, (c) Sb 3d, (d) Br 3d, (e) Si 2p, and (f) O 1s of MCM-41, bulk CBSB-0.3, and 50% MCM-41@CBSB-0.3.

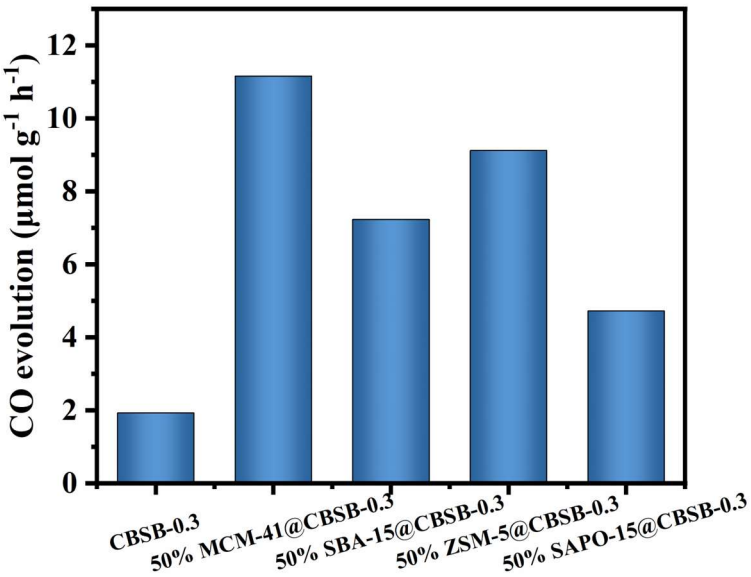

Fig. S14. The photocatalytic performance of CBSB-0.3 and series molecular sieves@CBSB-0.3.

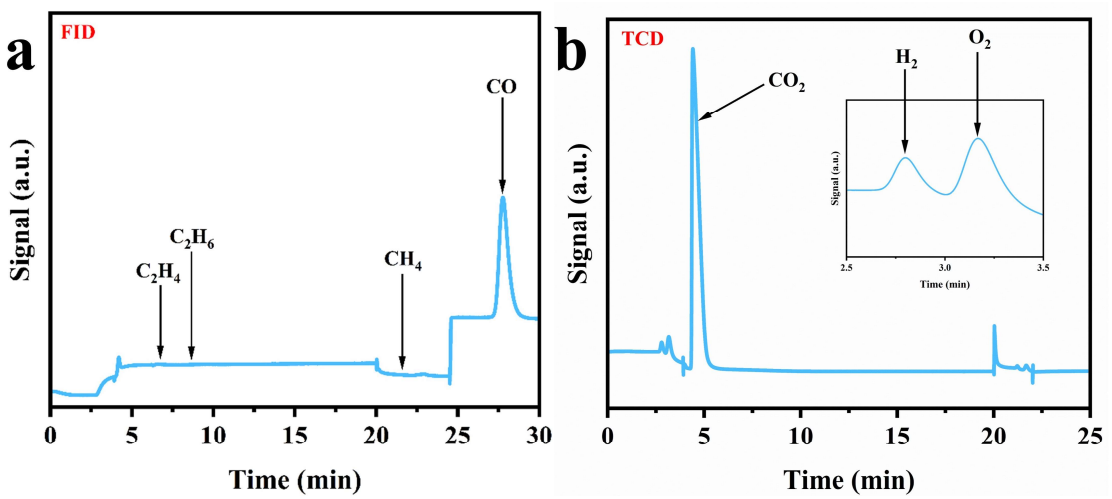

Fig. S15. Retention time distribution of different products detected by the thermal conductivity cell detector channel of GC after light irradiation for 4 h.

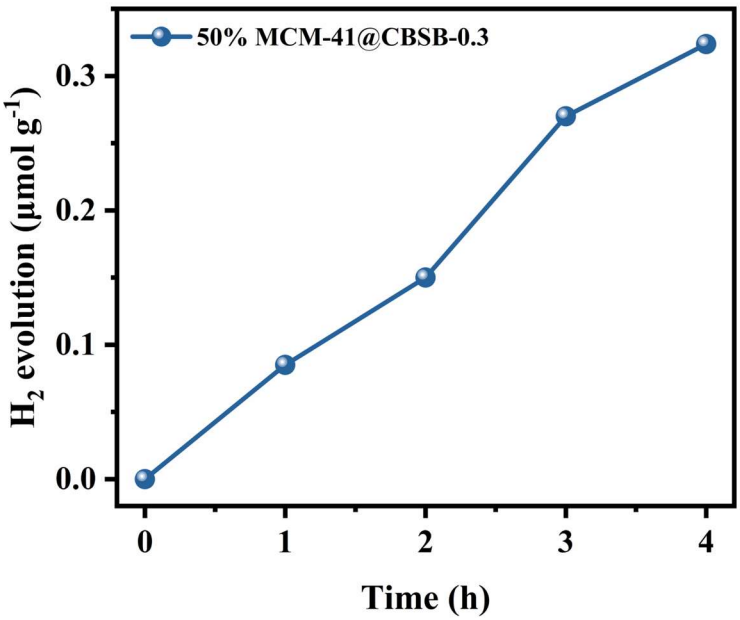

Fig. S16. H_2 production of 50% MCM-41@CBSB-0.3 during photocatalytic CO_2 reduction.

Table S1. Comparison of the specific surface areas and average pore sizes of CBSB-0.3, MCM-41, and a series of MCM-41@CBSB-0.3.

Sample	S_{BET} (m^2 g^{-1})	Average pore size (nm)
CBSB-0.3	3.8	14.4
30% MCM-41@CBSB-0.3	181.9	3.3
50% MCM-41@CBSB-0.3	220.3	3.4
70% MCM-41@CBSB-0.3	506.1	2.9
MCM-41	817.6	2.4

Table S2. Comparison of the photocatalytic CO_2 reduction reaction activity of reported photocatalysts under different reaction conditions.

Catalysts	Reaction conditions	CO yield / μmol g^{-1} h^{-1}	Light	Reference
$CsPbBr_3$ Qd	ethyl acetate/water (0.3%)	0.6	AM 1.5G	[1]
$CsPbBr_3$@ZIF-67	Gas-solid	0.77	AM 1.5G	[2]
$CsAgBiBr_6$	Ethyl acetate	2.3	AM 1.5G	[3]
$Cs_3Bi_2I_9$	Gas-solid	7.76	UV，305nm	[4]
Fe(II)-doped $CsPbBr_3$	Gas-solid	3.2	Xe lamp	[5]
$Cs_3Bi_2I_9/Bi_2WO_6$	Gas-solid	7.3	Xe lamp	[6]
g-C_3N_4/$BiVO_4$	Gas-solid	1.75	Xe lamp, ≥ 400nm	[7]
$NiAl_2O_4$/g-C_3N_4	Gas-solid	10.73	Xe lamp	[8]
$BiO_{1-x}Br$/g-C_3N_4	Water	13.11	Xe lamp, ≥420nm	[9]
50% MCM-41@CBSB-0.3	Gas-solid	11.2	Xe lamp, >420nm	This work

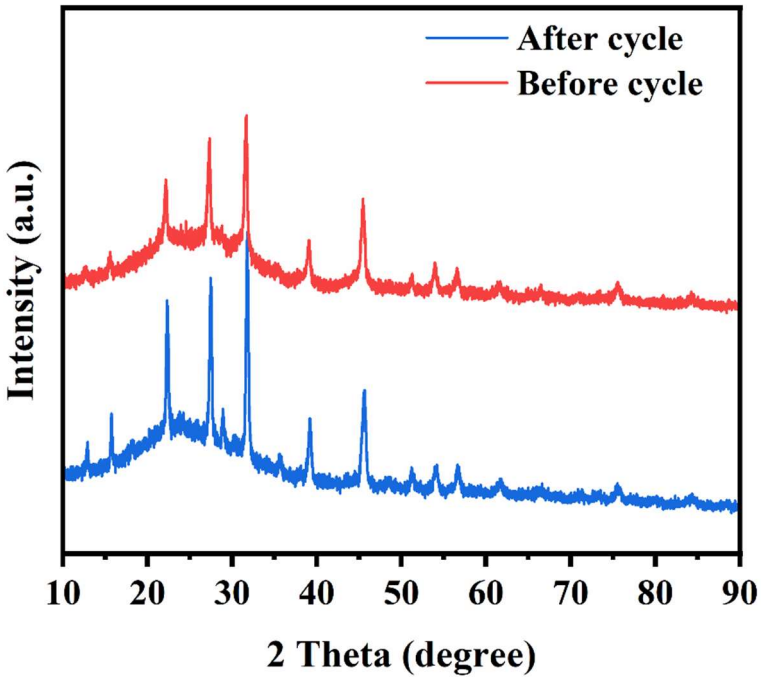

Fig. S17. Comparison of XRD patterns of 50% MCM-41@CBSB-0.3 sample before and after cycling reaction.

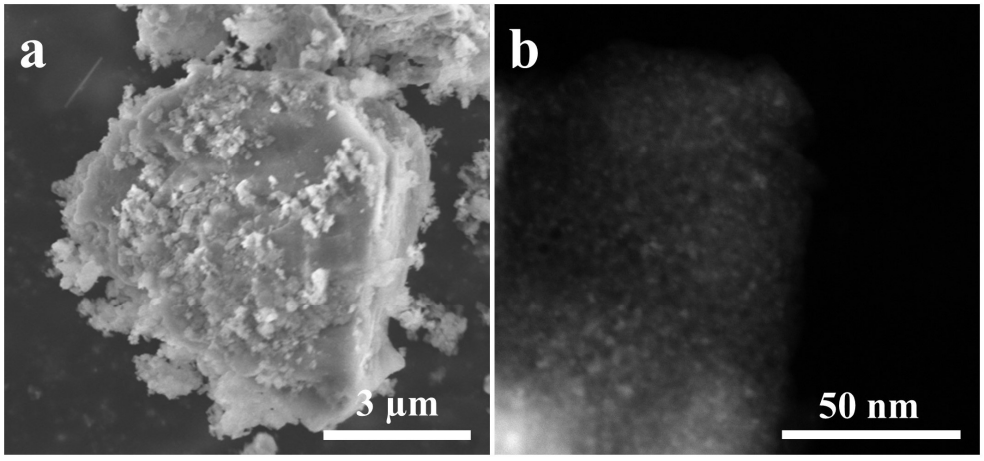

Fig. S18. (a) SEM images and (b) TEM images of 50% MCM-41@CBSB-0.3 after cycle.

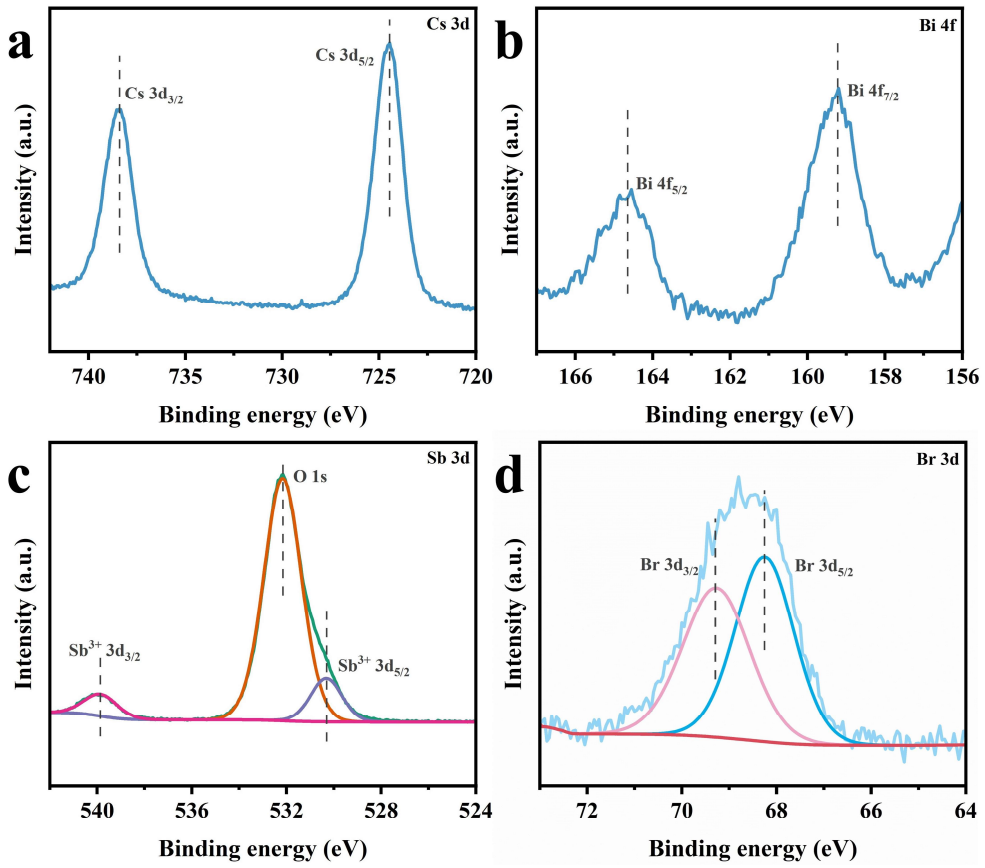

Fig. S19. XPS spectra of (a) Cs 3d, (b) Bi 4f, (c) Sb, and (d) Br 3d of 50% MCM-41@CBSB-0.3 after cycle.

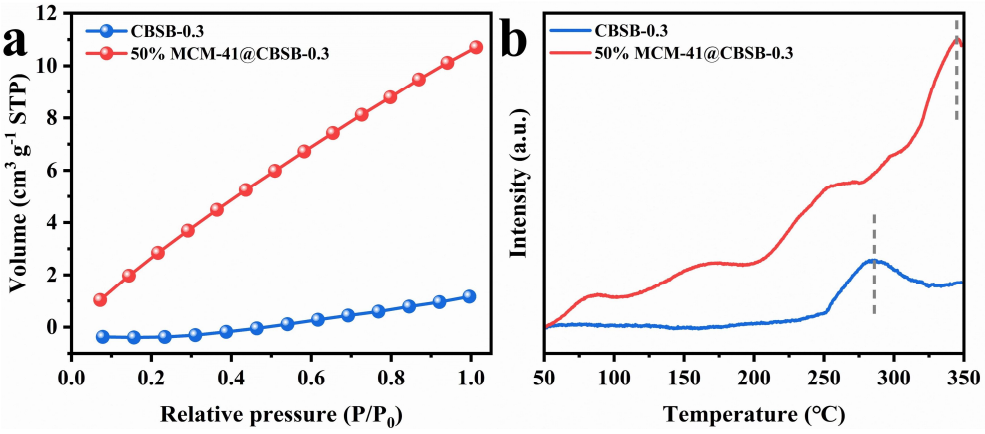

Fig. S20. (a) The CO_2 adsorption isotherm curves of MCM-41, CBSB-0.3, and 50% MCM-41@CBSB-0.3. (b) CO_2-TPD of CBSB-0.3 and 50% MCM-41@CBSB-0.3.

Table S3. Fitted PL decay parameters of CBSB-0.3 and 50% MCM-41@CBSB-0.3.

Sample	B_1	τ_1 (ns)	B_2	τ_2 (ns)	$\tau_{average}$ (ns)
CBSB-0.3	881.53	1.39	46.08	9.79	1.81
50% MCM-41@CBSB-0.3	51.34	1.63	955.72	1.91	2.64

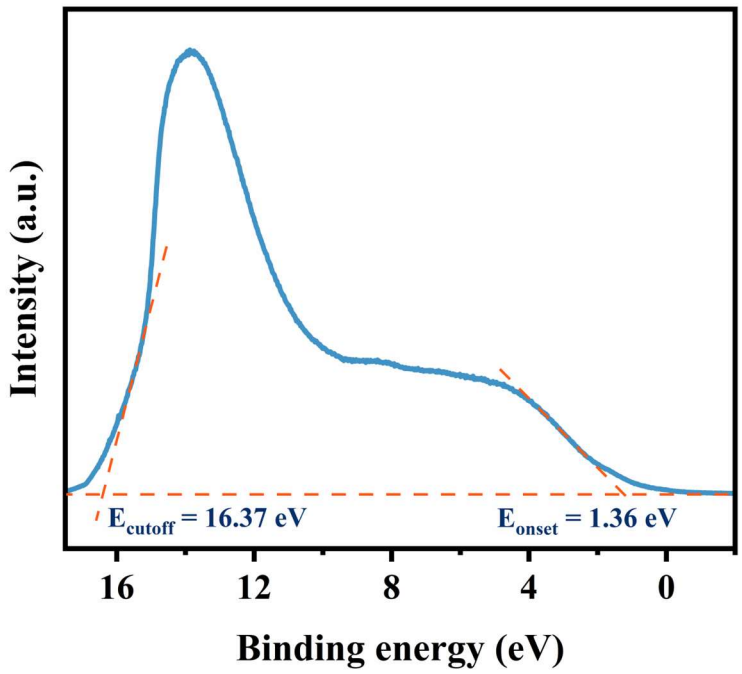

Fig. S21. UPS valence band spectra of 50% MCM-41@CBSB-0.3.

Reference

[1] J. Hou, S. Cao, Y. Wu, Z. Gao, F. Liang, Y. Sun, Z. Lin and L. Sun, *Chemistry*, 2017, **23**, 9481.

[2] Z.C. Kong, J.F. Liao, Y.J. Dong, Y.F. Xu, H.Y. Chen, D.B. Kuang and C.Y. Su, *ACS Energy. Lett.*, 2018, **3**, 2656-2662.

[3] L. Zhou, Y.F. Xu, B.X. Chen, D.B. Kuang and C.Y. Su, *Small*, 2018, **14**, 1703762.

[4] Y.Y. Wang, Q.X. Zhou, Y.F. Zhu and D.S. Xu, *Appl. Catal. B Environ.*, 2021, **294**, 120236.

[5] S. Shyamal, S.K. Dutta and N. Pradhan, *J. Phys. Chem. Lett.*, 2019, **10**, 7965-7969.

[6] Z.L. Liu, R.R. Liu, Y.F. Mu, Y.X. Feng, G.X. Dong, M. Zhang and T.B. Lu, *Sol. Rrl.*, 2021, **5**, 2000691.

[7] G. Zhou, L. Meng, X. Ning, W. Yin, J. Hou, Q. Xu, J. Yi, S. Wang and X. Wang, Intl. J. *Hydrog. Energy.*, 2022, **47**, 8749-8760.

[8] N. Ahmad, C. J. Kuo, M. Mustaqeem, M. K. Hussien and K. Chen, *Mater. Today. Phys.*, 2023, **31**, 100965.

[9] X. M. Jia, H. Y. Sun, H. L. Lin, J. Cao, C. Hu and S. F. Chen, *Appl. Surf. Sci.*, 2023, **614** 156017.